Received: 3 August 2022 | Revised: 18 January 2023 | Accepted: 31 January 2023

DOI: 10.1002/mp.16304

RESEARCH ARTICLE

MEDICAL PHYSICS

# Patient-specific fetal radiation dosimetry for pregnant patients undergoing abdominal and pelvic CT imaging

**Shuiyin Qu**[1,2] | **Haikuan Liu**[1] | **Tianwu Xie**[1,3] | **Maryellen L. Giger**[4] | **Guotao Quan**[5] | **Habib Zaidi**[3,6,7,8]

[1]Institute of Radiation Medicine, Fudan University, Shanghai, China

[2]Department of Engineering Physics, Tsinghua University, Beijing, China

[3]Division of Nuclear Medicine and Molecular Imaging, Geneva University Hospital, Geneva, Switzerland

[4]University of Chicago, Department of Radiology, Committee on Medical Physics, Chicago, Illinois, USA

[5]Shanghai United Imaging Intelligence Co., Ltd., Shanghai, China

[6]Geneva Neuroscience Center, Geneva University, Geneva, Switzerland

[7]Department of Nuclear Medicine and Molecular Imaging, University of Groningen, University Medical Center Groningen, Groningen, Netherlands

[8]Department of Nuclear Medicine, University of Southern Denmark, Odense, Denmark

**Correspondence**
Tianwu Xie, Fudan University, Institute of Radiation Medicine, 2094 Xietu Road, Shanghai 200032, China.
Email: tianwuxie@fudan.edu.cn

**Funding information**
National Natural Science Foundation of China, Grant/Award Number: 32227801; Swiss National Science Foundation, Grant/Award Number: SNSF 320030_176052

## Abstract

**Background:** Accurate estimation of fetal radiation dose is crucial for risk-benefit analysis of radiological imaging, while the radiation dosimetry studies based on individual pregnant patient are highly desired.

**Purpose:** To use Monte Carlo calculations for estimation of fetal radiation dose from abdominal and pelvic computed tomography (CT) examinations for a population of patients with a range of variations in patients' anatomy, abdominal circumference, gestational age (GA), fetal depth (FD), and fetal development.

**Methods:** Forty-four patient-specific pregnant female models were constructed based on CT imaging data of pregnant patients, with gestational ages ranging from 8 to 35 weeks. The simulation of abdominal and pelvic helical CT examinations was performed on three validated commercial scanner systems to calculate organ-level fetal radiation dose.

**Results:** The absorbed radiation dose to the fetus ranged between 0.97 and 2.24 mGy, with an average of 1.63 ± 0.33 mGy. The $CTDI_{vol}$-normalized fetal dose ranged between 0.56 and 1.30, with an average of 0.94 ± 0.25. The normalized fetal organ dose showed significant correlations with gestational age, maternal abdominal circumference (MAC), and fetal depth. The use of ATCM technique increased the fetal radiation dose in some patients.

**Conclusion:** A technique enabling the calculation of organ-level radiation dose to the fetus was developed from models of actual anatomy representing a range of gestational age, maternal size, and fetal position. The developed maternal and fetal models provide a basis for reliable and accurate radiation dose estimation to fetal organs.

**KEYWORDS**
computational model, CT, fetal radiation dose, Monte Carlo, pregnant patients

## 1 | INTRODUCTION

Pregnant females might be exposed to ionizing radiation during radiological procedures performed for clinical diagnosis of acute abdominal pain, trauma cancer and a number of other clinical indications. As the embryo/fetus presents significantly higher radiosensitivity than adults,[1] the International Commission on Radiological Protection (ICRP) reported that radiation doses above 100 mGy may lead to deterministic effects to the fetus, such as malformation, death, and mental retardation.[2] In addition, the ICRP publication 103 suggested that fetal radiation doses lower than 100 mGy cannot be used as an argument to stop pregnancy, a decision that should be carefully studied from different perspectives.[3] It is important to estimate fetal organ doses from diagnostic radiological examinations to understand the risks to the developing fetus from ionizing radiation. Due to ethical concerns, the fetal radiation dose can hardly be directly measured and has become a challenge for medical physicists.

Shuiyin Qu and Haikuan Liu contributed equally to the work.

  

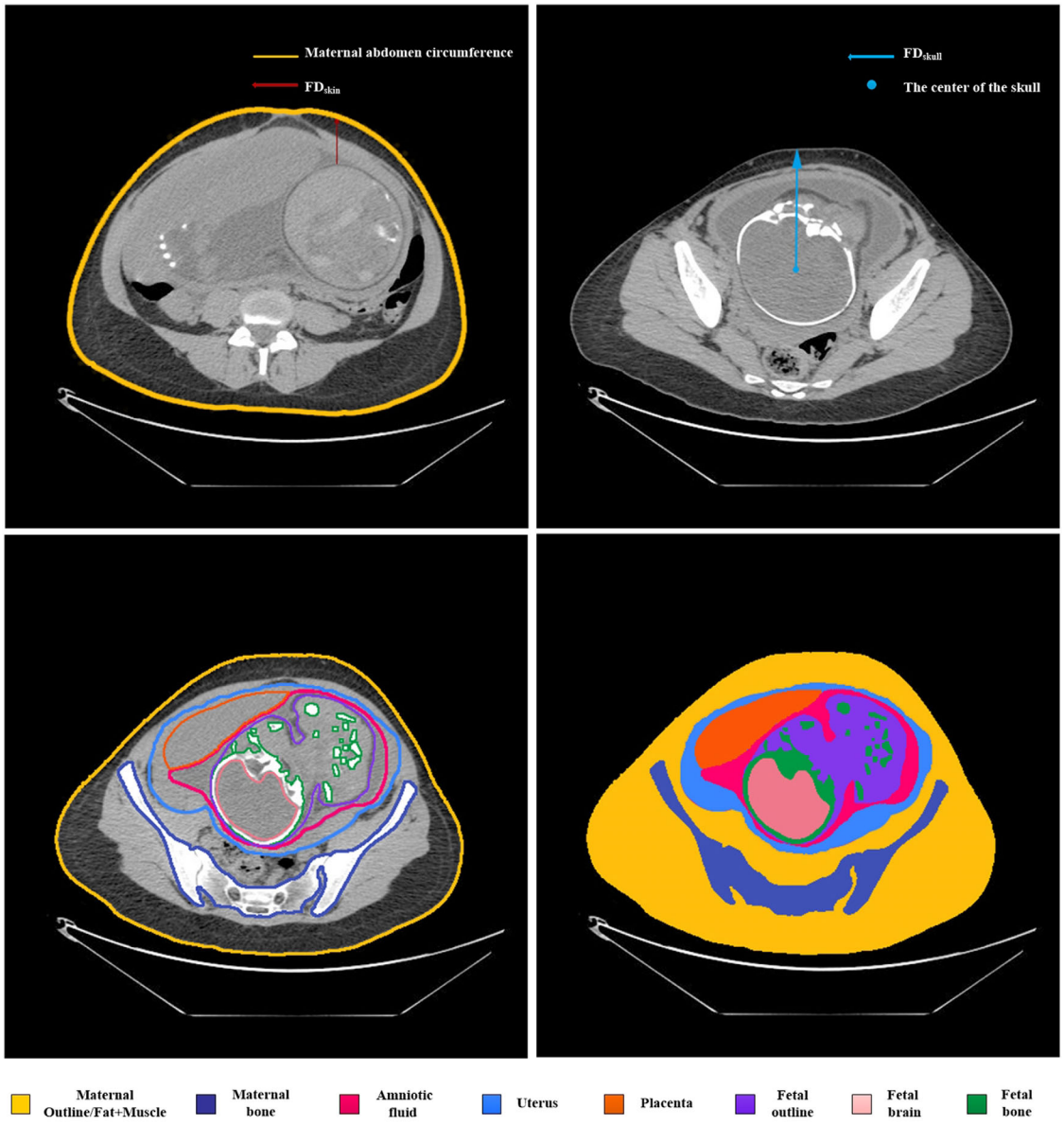


**FIGURE 1** CT images of a pregnant female patient at 35 weeks of gestation showing the segmented organs and measurements of maternal abdominal circumference, fetal skin depth ($FD_{skin}$), and fetal skull depth ($FD_{skull}$) distances.

A number of studies have reported on the use of Monte Carlo (MC) simulations to estimate fetal radiation dose,[4–10] where fetal dosimetry was performed using a reference model or a maternal-size-adjusted reference model without including the individual anatomical characteristics of the fetus, hence introducing an extra error in radiation dosimetry.[4] For example, Maynard et al.[11] constructed eight reference models for pregnant women. The ICRP Publication 145[12] also published a series of mesh-type reference computational phantoms. With the increasing interest in personalized radiation dosimetry among the scientific community, the construction of personalized computational models has become popular.[13,14] Angel et al.[15] constructed patient-specific voxel models for 24 pregnant patients for fetal dose calculation in abdominal CT examinations, but the fetal organ-level radiation dose was immeasurable because of the limited number of identified fetal organs. Since the radiosensitivity and radiation risks of developing fetal organs vary across the different gestational ages, organ-scale radiation dosimetry for the fetus is crucial and highly desired for epidemiological studies aiming to correlate between conceptus radiation exposure and organ-specific childhood cancer after birth. In addition, most of the aforementioned previous work was performed using fixed tube current (FTC) acquisition protocols. As automatic tube current-modulated (ATCM) CT scanning becomes popular, it is important to

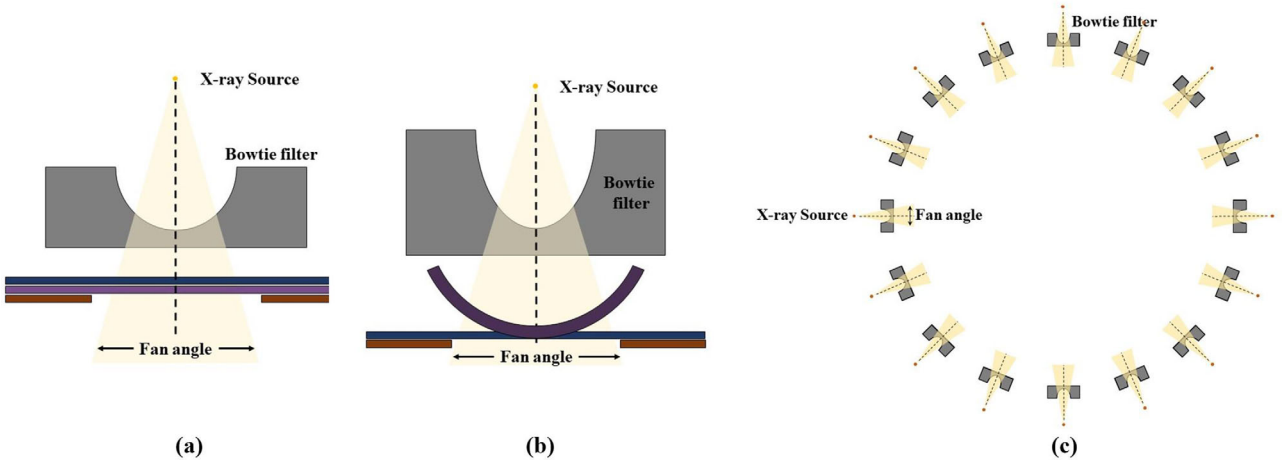


**FIGURE 2** Geometry of three validated commercial CT scanner models: (a) GE Discovery CT 750 HD scanner, (b) Siemens SOMATOM Definition Edge scanner, and (c) United Imaging Healthcare uCT 760 128-slice CT scanner.

estimate fetal dose from different scanning protocols across a variety of CT scanners.

In this work, we constructed a series of pregnant female models at different gestational ages based on CT images of real patients and performed MC simulations to calculate the radiation dose delivered to the fetus. Three previously validated CT scanner systems, including the GE Discovery CT 750 HD, the Siemens SOMATOM Definition Edge, and the United Imaging Healthcare uCT 760 128-slice CT, were incorporated into the MC simulations. The fetal radiation dose from abdominal/pelvic CT examinations on five scanners, including the Siemens SOMATOM Force, the Philips Brilliance 40, the Siemens Definition AS, the GE LightSpeed VCT, and the GE Discovery CT750 HD, were calculated and compared. The correlations between fetal organ dose from CT examinations and various attributes such as scanning protocols, individual anatomical characteristics, gestational age, intra-uterine position, and fetal size were investigated.

## 2 | MATERIALS AND METHODS

### 2.1 | Patient-specific computational models

A total of 44 patient-specific computational models were constructed based on clinical CT images of pregnant patients acquired at Geneva University Hospital (HUG), Switzerland. These patients were initially admitted to the emergency department of HUG because of acute abdominal pain and underwent ultrasound examinations upon admission, which however did not yield an etiology or conclusive diagnosis. MRI examination was not possible either owing to lack of slots or patients presenting very late in the evening. Hence, the patients underwent abdominal and pelvic low-dose CT examinations. CT images of pregnant patients were segmented using Photoshop software (San Jose, California, USA), while the NURBS-based organ surfaces were reconstructed using Rhinoceros software (Seattle, Washington, USA). The construction of patient-specific computational models for pregnant females based on clinical CT images has been described in detail in the prior article.[16] This prior article dealt with development of digital fetus library and the measurement of anatomical parameters, whereas in this manuscript, we report on the radiation dosimetry study for fetus and pregnant patient in abdominal and pelvic CT examinations. The measured anatomical parameters include femoral length (FL), humerus length (HL), biparietal diameter (BPD), head circumference (HC), abdominal circumference (FAC), fetal skin depth ($FD_{skin}$), and fetal skull depth ($FD_{skull}$). The constructed abdominal models of pregnant female subjects were named Maternal_Abdominal_Model-X (MAM-X) where *X* refers to the model ID. Figure 1 illustrates the manual methods of image segmentation and measurements of the maternal abdominal circumference and intra-uterine position of $FD_{skin}$ and $FD_{skull}$. MAC was taken as the circumference of the pregnant woman's belly button, while $FD_{skin}$ and $FD_{skull}$ were calculated as the shortest distances between the most front of the fetal skin and the 3D center of the fetal skull to the skin surface of the pregnant woman, respectively. All above-mentioned feature points and data were measured using the Rhinoceros software.

### 2.2 | Monte Carlo simulation and radiation dose calculations

The study included three clinical CT scanner systems, namely, a GE Discovery CT 750 HD scanner,[4,17] a

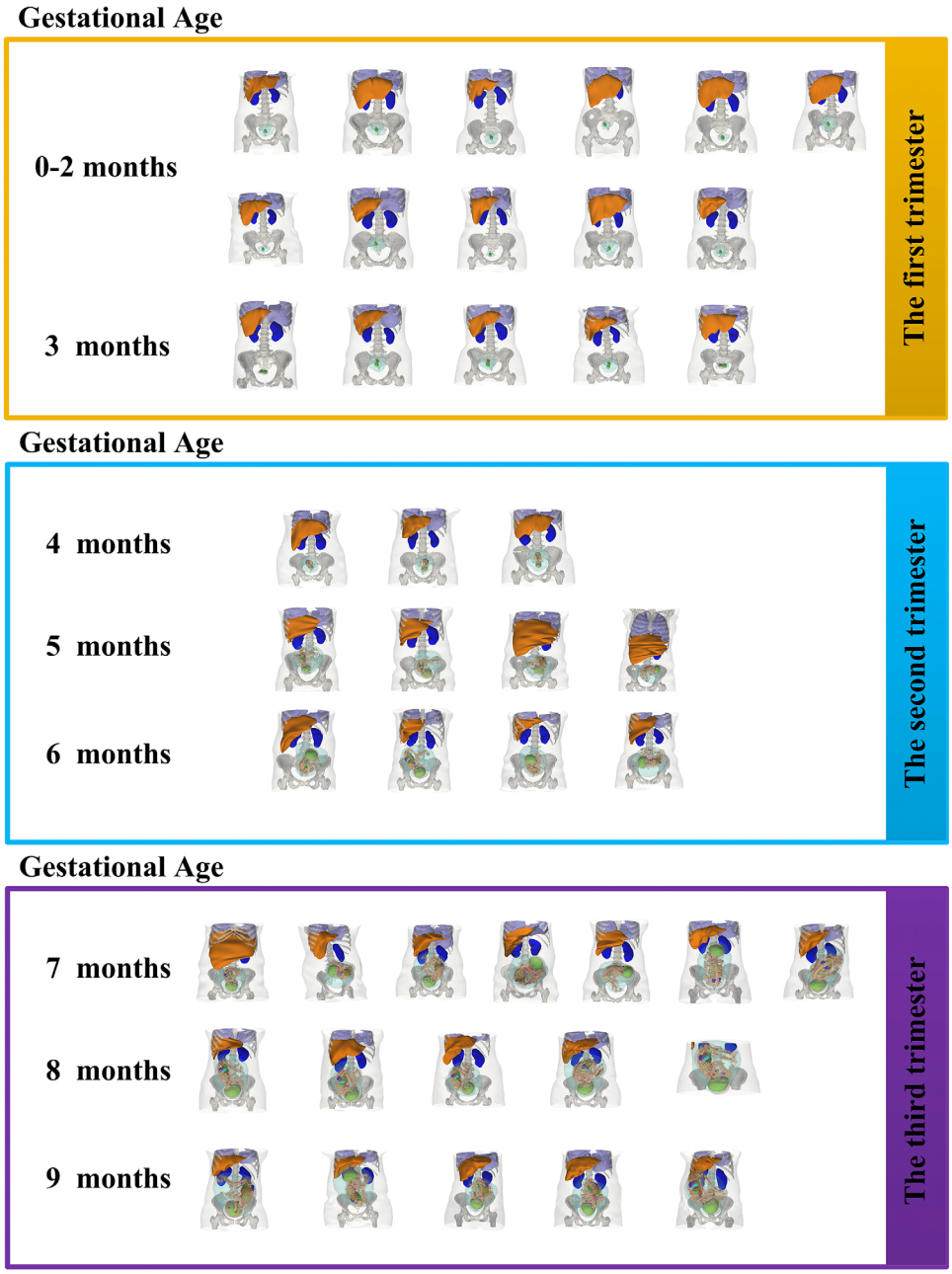


**FIGURE 3** 3D visualization of the developed patient-specific computational phantoms at different gestational ages/trimesters. The outer outline of pregnant patients and the uterus are transparent for better visualization of internal organs.

Siemens SOMATOM Definition Edge scanner,[18] and a the United Imaging Healthcare uCT 760 128-slice CT scanner,[19] which had been previously incorporated into the MCNPX Monte Carlo code[20] for calculations of radiation dose of various organs, however, not for pregnant patients. The geometries of the three CT gantries, including the source to detector distance, focal spot size, fan angle, etc., had been taken into account in the simulation of corresponding CT scanners as shown in Figure 2. Simulations of x-ray photon transport were performed to yield dose calculations based on 44 pregnant-female phantoms where the fetal radiation dose refers to the total deposited energy in the fetal body divided by the body weight of the fetus. For each phantom, the simulated energy deposition in 25 fetal organs and maternal body were recorded and used for the radiation dosimetry calculations. For each patient phantom and for each organ, the simulated radiation doses were averaged across all three simulated CT scanners. The detailed data processing and correlation analysis methods are provided in Supplemental Materials.

**TABLE 1** Anatomical measurements for 44 pregnant patients and their fetuses.

| Model Number | GA (weeks) | MAC (cm) | CT scanners | Mean $CTDI_{vol}$ (mGy) | Mean effective mAs | Scan length (cm) | FL (mm) | HL (mm) | BPD (mm) | HC (mm) | FAC (mm) | $FD_{skull}$ (mm) | $FD_{skin}$ (mm) |
|---|---|---|---|---|---|---|---|---|---|---|---|---|---|
| MAM-1 | 8 | 84.63 | GE Discovery CT750 HD | 1.78 | 22.88 | 42.5 | – | – | – | – | – | – | – |
| MAM-2 | 8 | 79.35 | GE Discovery CT750 HD | 1.78 | 22.88 | 41.5 | – | – | – | – | – | – | – |
| MAM-3 | 8 | 76.90 | GE Discovery CT750 HD | 1.78 | 22.88 | 41.9 | – | – | – | – | – | – | – |
| MAM-4 | 8 | 70.40 | GE Discovery CT750 HD | 1.78 | 22.88 | 45.5 | – | – | – | – | – | – | – |
| MAM-5 | 8 | 78.98 | Philips Brilliance 40 | 9.59 | 162.51 | 47.3 | – | – | – | – | – | – | – |
| MAM-6 | 8 | 94.09 | GE Discovery CT750 HD | 1.78 | 22.88 | 47.5 | – | – | – | – | – | – | – |
| MAM-7 | 8 | 98.46 | GE Discovery CT750 HD | 1.78 | 22.88 | 44.5 | – | – | – | – | – | – | – |
| MAM-8 | 8 | 80.99 | GE Discovery CT750 HD | 1.78 | 22.88 | 41.5 | – | – | – | – | – | – | – |
| MAM-9 | 8 | 93.33 | GE Discovery CT750 HD | 1.78 | 22.88 | 49.9 | – | – | – | – | – | – | – |
| MAM-10 | 8 | 86.13 | GE Discovery CT750 HD | 1.78 | 22.88 | 41.5 | – | – | – | – | – | – | – |
| MAM-11 | 8 | 117.80 | GE Discovery CT750 HD | 1.78 | 22.88 | 43.9 | – | – | – | – | – | – | – |
| MAM-12 | 10 | 119.00 | GE Discovery CT750 HD | 1.78 | 22.88 | 50.5 | – | – | 8.69 | 33.5 | – | – | – |
| MAM-13 | 10 | 77.58 | GE Discovery CT750 HD | 1.78 | 22.88 | 43.5 | – | – | 8.87 | 32.8 | – | – | – |
| MAM-14 | 10 | 93.25 | GE Discovery CT750 HD | 1.78 | 22.88 | 43.9 | – | – | 9.09 | 33.0 | – | – | – |
| MAM-15 | 12 | 98.99 | GE LightSpeed VCT | 1.81 | 22.90 | 47.9 | – | – | 9.11 | 32.7 | – | – | – |
| MAM-16 | 12 | 89.18 | SIEMENS Definition AS | 10.82 | 141.93 | 43.9 | – | – | 9.15 | 33.4 | – | – | – |
| MAM-17 | 15 | 89.28 | GE Discovery CT750 HD | 1.78 | 22.88 | 39.5 | 30.76 | 29.13 | 37.95 | 134.1 | – | – | – |
| MAM-18 | 15 | 122.30 | SIEMENS SOMATOM Force | 2.94 | 43.03 | 48.7 | 30.67 | 29.13 | 36.97 | 132.9 | – | – | – |
| MAM-19 | 16 | 108.30 | GE Discovery CT750 HD | 1.78 | 22.88 | 45.5 | 32.88 | 31.31 | 37.34 | 133.5 | – | – | – |
| MAM-20 | 17 | 92.04 | GE Discovery CT750 HD | 1.78 | 22.88 | 45.9 | 32.58 | 31.37 | 46.91 | 171.0 | 151.6 | 90.5 | 41.87 |
| MAM-21 | 18 | 82.09 | GE Discovery CT750 HD | 1.78 | 22.88 | 43.9 | 30.97 | 29.91 | 48.64 | 162.8 | 148.9 | 85.0 | 51.42 |
| MAM-22 | 20 | 111.00 | GE Discovery CT750 HD | 1.78 | 22.88 | 64.7 | 34.93 | 33.33 | 53.25 | 175.9 | 202.6 | 119.7 | 63.71 |
| MAM-23 | 20 | 112.60 | GE Discovery CT750 HD | 1.78 | 22.88 | 47.9 | 34.23 | 34.75 | 51.65 | 193.1 | 189.3 | 116.0 | 68.81 |
| MAM-24 | 21 | 89.33 | GE Discovery CT750 HD | 1.78 | 22.88 | 41.3 | 36.04 | 34.62 | 52.15 | 184.4 | 179.2 | 82.9 | 38.36 |
| MAM-25 | 21 | 87.93 | GE Discovery CT750 HD | 1.78 | 22.88 | 37.9 | 31.92 | 32.94 | 52.70 | 188.1 | 158.0 | 88.7 | 58.28 |

(Continues)

**TABLE 1** (Continued)

| Model Number | GA (weeks) | MAC (cm) | CT scanners | Mean $CTDI_{vol}$ (mGy) | Mean effective mAs | Scan length (cm) | FL (mm) | HL (mm) | BPD (mm) | HC (mm) | FAC (mm) | $FD_{skull}$ (mm) | $FD_{skin}$ (mm) |
|---|---|---|---|---|---|---|---|---|---|---|---|---|---|
| MAM-26 | 22 | 101.90 | GE Discovery CT750 HD | 1.78 | 22.88 | 46.3 | 42.87 | 39.84 | 64.51 | 218.8 | 202.1 | 92.2 | 54.89 |
| MAM-28 | 23 | 98.08 | SIEMENS SOMATOM Force | 1.51 | 22.17 | 47.9 | 46.64 | 43.25 | 68.00 | 233.2 | 229.6 | 96.8 | 40.11 |
| MAM-29 | 25 | 109.50 | GE Discovery CT750 HD | 1.78 | 22.88 | 46.5 | 68.97 | 64.31 | 94.13 | 321.8 | 349.2 | 106.5 | 24.59 |
| MAM-30 | 25 | 92.21 | GE Discovery CT750 HD | 1.78 | 22.88 | 46.5 | 45.82 | 39.48 | 69.19 | 230.9 | 233.9 | 73.1 | 30.09 |
| MAM-31 | 25 | 96.01 | GE LightSpeed VCT | 1.81 | 22.90 | 46.9 | 58.82 | 54.92 | 83.68 | 300.7 | 277.6 | 77.6 | 37.59 |
| MAM-32 | 25 | 116.10 | GE Discovery CT750 HD | 1.78 | 22.88 | 47.5 | 46.39 | 43.31 | 63.81 | 232.9 | 242.6 | 173.9 | 61.45 |
| MAM-33 | 26 | 111.60 | GE Discovery CT750 HD | 1.78 | 22.88 | 44.9 | 57.28 | 52.49 | 75.75 | 261.5 | 248.3 | 101.9 | 47.62 |
| MAM-34 | 26 | 114.00 | GE LightSpeed VCT | 1.81 | 22.90 | 49.9 | 49.51 | 40.24 | 66.86 | 245.1 | 211.4 | 132.0 | 84.73 |
| MAM-35 | 28 | 88.92 | GE Discovery CT750 HD | 1.78 | 22.88 | 43.9 | 55.96 | 51.31 | 76.38 | 263.5 | 242.8 | 63.2 | 19.80 |
| MAM-36 | 29 | 127.90 | GE LightSpeed VCT | 1.81 | 22.90 | 48.1 | 62.93 | 58.70 | 83.24 | 278.7 | 264.1 | 149.5 | 78.27 |
| MAM-37 | 29 | 89.20 | GE Discovery CT750 HD | 1.78 | 22.88 | 47.5 | 56.15 | 48.33 | 78.33 | 289.3 | 256.7 | 71.2 | 22.89 |
| MAM-39 | 30 | 97.68 | GE Discovery CT750 HD | 1.78 | 22.88 | 42.9 | 61.75 | 51.21 | 82.56 | 285.6 | 257.4 | 92.9 | 22.71 |
| MAM-41 | 32 | 114.10 | GE Discovery CT750 HD | 1.78 | 22.88 | 48.5 | 64.51 | 61.12 | 88.30 | 309.3 | 278.3 | 124.0 | 40.84 |
| MAM-42 | 33 | 118.20 | GE Discovery CT750 HD | 1.78 | 22.88 | 46.9 | 60.91 | 55.62 | 85.05 | 296.2 | 244.5 | 117.4 | 46.23 |
| MAM-43 | 33 | 124.50 | GE Discovery CT750 HD | 1.78 | 22.88 | 48.3 | 61.20 | 55.62 | 85.65 | 295.3 | 239.8 | 158.9 | 52.17 |
| MAM-44 | 35 | 106.10 | GE Discovery CT750 HD | 1.78 | 22.88 | 42.5 | 72.68 | 56.65 | 88.53 | 321.9 | 332.6 | 143.5 | 46.92 |
| MAM-45 | 35 | 108.60 | GE Discovery CT750 HD | 1.78 | 22.88 | 47.9 | 65.95 | 55.79 | 84.75 | 311.7 | 309.2 | 116.3 | 44.88 |
| MAM-46 | 35 | 98.80 | GE LightSpeed VCT | 1.81 | 22.90 | 48.3 | 67.54 | 58.31 | 97.02 | 341.5 | 327.7 | 104.6 | 35.1 |

### 2.3 | Fetal dose from automatic tube current modulation (ATCM)

With the advancements of ATCM on modern CT scanners, protocols using this technology have become more widely adopted in the clinical setting. Four pregnant patients underwent CT scanning with ATCM and were thus further investigated in a pilot study. This includes patient MAM-5 scanned on Philips Brilliance 40 at the first trimester, patient MAM-16 scanned on Siemens Definition AS at the first trimester, and patients MAM-18 and MAM-28 scanned on Siemens SOMATOM Force at the second trimester. An in-house MATLAB code was used to derive the tube current modulation at each slice from the DICOM images. The extracted slice-specific tube currents were used for the calculation of radiation dose at each layer. The fetal organ dose was obtained by summing the radiation doses for each simulated layer.

## 3 | RESULTS

### 3.1 | Patient-specific fetal phantom

Figure 3 illustrates the 3D digital constructed maternal phantoms and Table 1 presents the measured anatomical parameters for each patient. The GA ranged from

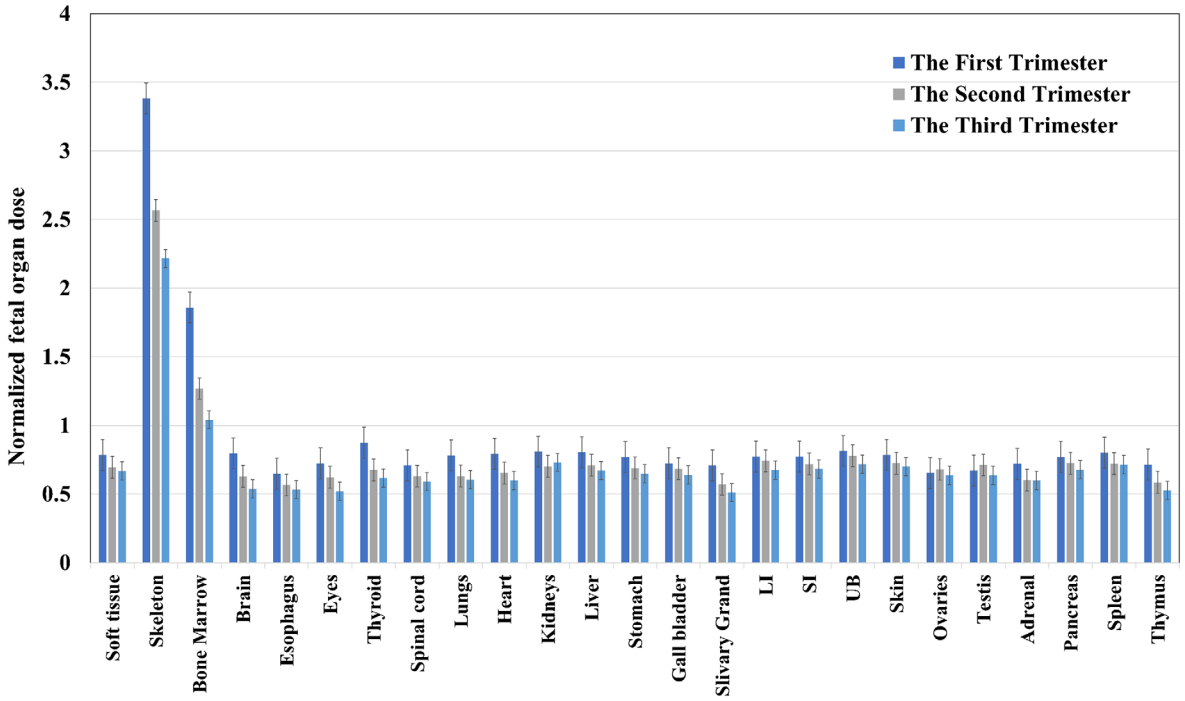


**FIGURE 4** Comparison of normalized fetal organ doses (average of three CT scanners and expressed as mean ± SD) at different gestational ages.

8 to 35 weeks. The abdominal circumference of pregnant patients varied between 70.4 and 127.9 cm with a median of 98.27 cm. The scan length of the pregnant woman accepted CT ranges between 23.7 and 64.7 cm. The minimum and maximum FAC were 148.9 and 349.2 mm, respectively. The FL, HL, BPD, and HC were within ranges 27.88-72.68 , 26.01-64.31 , 8.69-97.02, and 32.71-341.54 mm, respectively. The ranges of $FD_{skin}$ were from 19.80 to 84.73 mm, while $FD_{skull}$ varied from 63.22 to 173.90 mm.

## 3.2 | Fetal organ doses

The fetal organ doses from the three simulated CT scanner systems were estimated and normalized by dividing absorbed dose by the measured $CTDI_{vol}$ of each scanner. Figure 4 shows the calculated normalized fetal organ doses at different trimesters of pregnancy. Consistent with result reported in the literature, it was observed that the fetal organ dose decreases gradually with increasing gestational age.[15] The absorbed doses to the fetal skeleton and bone marrow were about 3.77 and 1.92 times higher than that of fetal soft-tissue. Table 2 shows the correlations between normalized fetal organ dose and the measured anatomical parameters, in which stepwise multiple linear regression analysis was used. As shown in Figure 5, significant correlations were observed between fetal organ dose and MAC, gestational age (GA), and FDs, while we failed to show statistical correlations between fetal organ dose and FAC, FL, HL, BPD, HC, and scan length. Linear fitting of fetal organ dose was performed for MAC, GA, and $FD_{skin}$ with each point representing one organ in the fetus of an individual patient.

To depict the variability of radiation doses among the three simulated CT scanners, the radiation dose to the fetal brain is compared in Figure 6. It can be observed that the absorbed dose decreases with MAC and the mean absolute dose difference between the developed CT models is 2.78%, thus indicating that the CTDIvol normalized absorbed dose may potentially be less affected by the different CT models than that reported by Turner et al.[26] The calculated average fetal organ doses from the three CT systems for skeleton, brain, kidney, liver, and body are shown in Figure 7. For pregnant patients undergoing CT examination, the radiation dose to the fetal skeleton and bone marrow are higher than other organs, whereas the dose to the fetal brain was the lowest. Radiation doses to other organs were found to be similar to each other.

## 3.3 | Fetal organ dose estimation model

As shown in Table 2, the fetal organ dose demonstrated statistically significant correlations with MAC, GA, and $FD_{skin}$. The measurements of MAC and GA for individual patients can be routinely obtained in clinical setting

**TABLE 2** Analysis of the correlation between different fetal organs and anatomical parameters in the three CT scanner models (* refers to $P < 0.005$).

| Tissue/ organs | MAC | | | GA | | | Fetal skull depth | | | Fetal skin depth | | |
|---|---|---|---|---|---|---|---|---|---|---|---|---|
| | Siemens | GE | United Imaging | Siemens | GE | United Imaging | Siemens | GE | United Imaging | Siemens | GE | United Imaging |
| Fetal soft tissue | −.853* | −.806* | −.873* | −.417* | −.315 | −.455* | −.778* | −.728* | −.788* | −.724* | −.741* | −.721* |
| Fetal skeleton | −.837* | −.830* | −.848* | −.720* | −.698* | −.737* | −.913* | −.905* | −.907* | −.500* | −.486* | −.508* |
| Fetus Bone Marrow | −.345 | −.295 | −.329 | −.273 | −.211 | −.255 | −.894* | −.899* | −.897* | −.429 | −.426 | −.451 |
| Fetus Brain | −.846* | −.833* | −.861* | −.664* | −.623* | −.676* | −.892* | −.879* | −.891* | −.413 | −.385 | −.440 |
| Fetus Esophagus | .187 | .235 | .193 | .556* | .604* | .563* | −.846* | −.802* | −.852* | −.606* | −.606* | −.618* |
| Fetus Eyes | −.816* | −.807* | −.837* | −.572* | −.548* | −.605* | −.745* | −.779* | −.771* | −.333 | −.376 | −.357 |
| Fetus Thyroid | −.325 | −.264 | −.310 | −.078 | .015 | −.066 | −.871* | −.834* | −.870* | −.501* | −.474 | −.509* |
| Fetus Spinal cord | .198 | .245 | .200 | .562* | .607* | .562* | −.762* | −.721* | −.787* | −.587* | −.585* | −.604* |
| Fetus Lungs | −.850* | −.810* | −.863* | −.554* | −.470* | −.577* | −.834* | −.777* | −.842* | −.643* | −.675* | −.656* |
| Fetus Heart | −.860* | −.841* | −.879* | −.598* | −.550* | −.617* | −.816* | −.780* | −.827* | −.550* | −.596* | −.578* |
| Fetus Kidneys | −.710* | −.616* | −.757* | −.236 | −.137 | −.294 | −.584* | −.458 | −.642* | −.682* | −.621* | −.707* |
| Fetus Liver | −.844* | −.787* | −.859* | −.466* | −.375* | −.482* | −.813* | −.733* | −.824* | −.577* | −.588* | −.594* |
| Fetus Stomach | −.746* | −.683* | −.769* | −.411* | −.329 | −.422* | −.529* | −.461 | −.554* | −.556* | −.540* | −.579* |
| Fetus Gallbladder | −.785* | −.676* | −.822* | −.372 | −.197 | −.392* | −.704* | −.603* | −.744* | −.415 | −.398 | −.475 |
| Fetus Slivary Grand | −.875* | −.862* | −.876* | −.605* | −.564* | −.628* | −.884* | −.894* | −.891* | −.516* | −.493* | −.513* |
| Fetus LI | −.755* | −.658* | −.792* | −.390* | −.253 | −.415* | −.568* | −.457 | −.609* | −.457 | −.418 | −.507* |
| Fetus SI | −.753* | −.652* | −.783* | −.348 | −.219 | −.369 | −.584* | −.479* | −.621* | −.537* | −.500* | −.575* |
| Fetus UB | −.686* | −.588* | −.749* | −.318 | −.196 | −.371 | −.485* | −.390 | −.531* | −.424 | −.385 | −.471 |
| Fetus Skin | −.842* | −.785* | −.871* | −.321 | −.194 | −.373* | −.838* | −.802* | −.839* | −.728* | −.740* | −.720* |
| Fetus Ovaries | .268 | .301 | .262 | .632* | .665* | .629* | −.542* | −.451 | −.584* | −.479* | −.455 | −.538* |
| Fetus Testis | .295 | .326 | .300 | .615* | .643* | .623* | −.389 | −.306 | −.449 | −.335 | −.326 | −.382 |
| Fetus Adrenal | −.791* | −.727* | −.814* | −.422* | −.323 | −.438* | −.692* | −.611* | −.724* | −.683* | −.678* | −.699* |
| Fetus Pancreas | −.739* | −.643* | −.778* | −.359 | −.229 | −.374* | −.532* | −.428 | −.585* | −.467 | −.433 | −.529* |
| Fetus Spleen | −.647* | −.544* | −.681* | −.284 | −.183 | −.309 | −.417 | −.340 | −.437 | −.547* | −.510* | −.578* |
| Fetus Thymus | −.871* | −.850* | −.884* | −.612* | −.570* | −.633* | −.862* | −.839* | −.874* | −.502* | −.499* | −.523* |

*At 0.005 level, the correlation is significant.

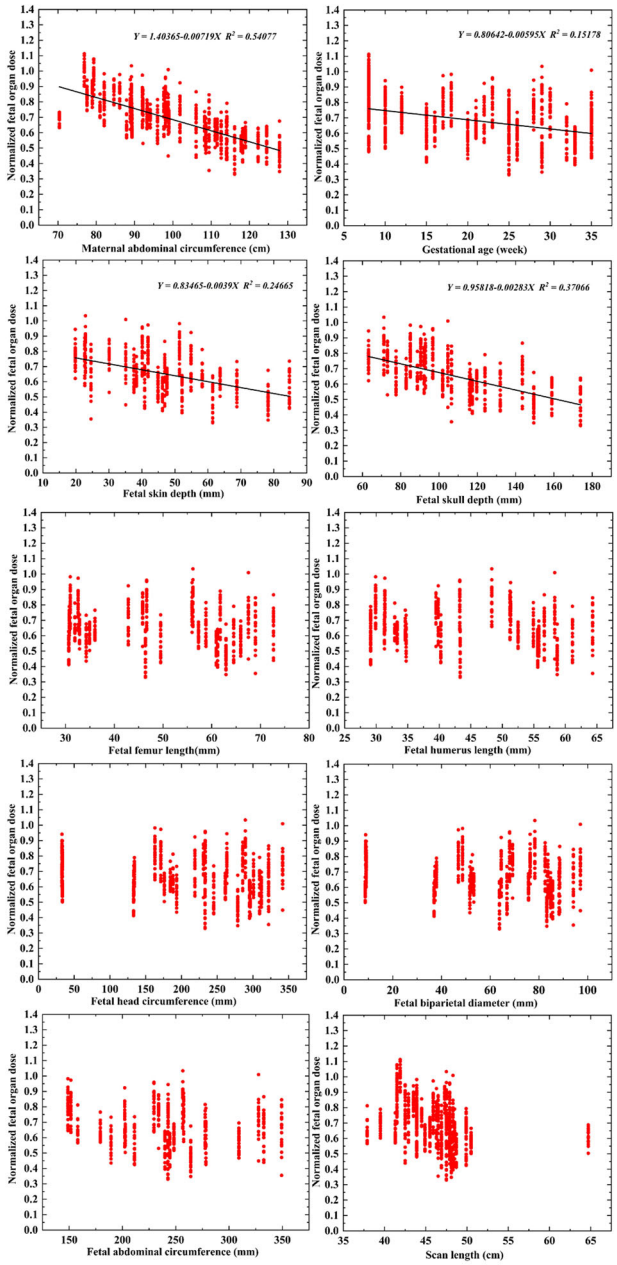


**FIGURE 5** Correlations between normalized fetal organ doses and measured anatomical parameters. Stepwise multiple linear regression was performed to analyze the correlation of fetal organ dose with MAC, GA, $FD_{skin}$, and $FD_{skull}$. The normalized fetal organ dose was averaged among three CT models.

without access to medical images, whereas $FD_{skin}$ can be measured from ultrasound examinations. From the initial 44 digital patient models investigated, two models incorporating the attainable attributes of MAC, GA, and $FD_{skin}$, for fetal organ dose estimation in abdominal and pelvic CT imaging were determined:

$$\text{Model I: } \textit{Normalized organ dose}_{I} = \alpha + \beta_1 \times MAC + \beta_2 \times GA \quad (1)$$

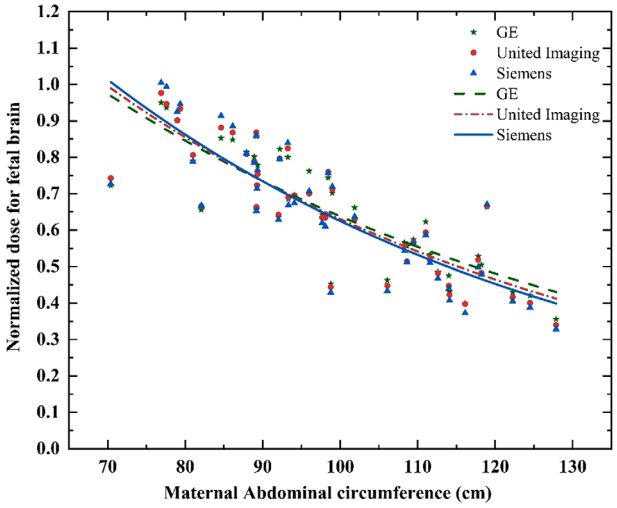


**FIGURE 6** Normalized radiation doses to the fetal brain for the three considered CT scanners.

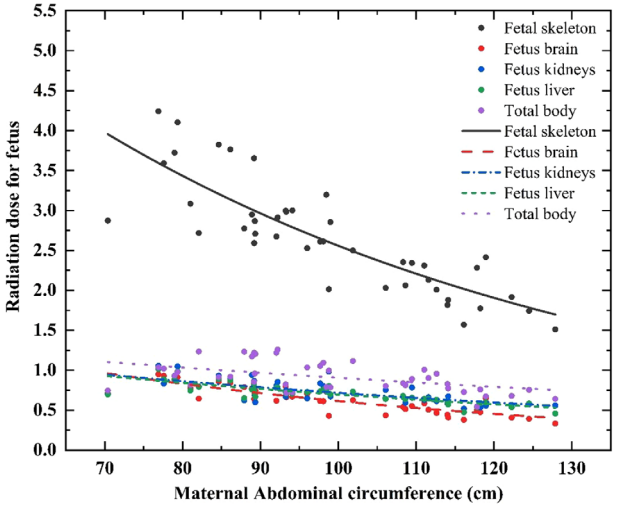


**FIGURE 7** The correlations between scanner-averaged normalized fetal organ doses with maternal abdominal circumference of pregnant patients for fetal skeleton, fetal brain, fetal kidney, fetal liver, and fetal body.

$$\text{Model II: } \textit{Normalized organ dose}_{II} = \alpha + \beta_1 \times MAC + \beta_2 \times GA + \beta_3 \times FD_{skin} \quad (2)$$

where the normalized organ dose refers to the fetal absorbed dose per $CTDI_{vol}$ in abdominal and pelvic CT examinations. Table 3 lists the determined mathematical form of dose estimation models for each fetal organ, while models presenting with $R^2 < 0.5$ were discarded. In most cases, three-factor models yielded better fit than two-factor models as indicated by a higher value of $R^2$. For example, the dose estimation formulas of Model II

for fetal total body can be calculated as:

$$\text{Normalized organ dose}_{II}\,(\text{fetal total body}) = 2.519 - 0.012 \times MAC - 0.01 \times GA - 0.001 \times FD_{skin},\ R^2 = 0.919$$

In specific abdominal CT examinations for pregnant female, the absolute radiation dose (in mGy) to the fetus can be calculated from the calculated normalized organ dose by:

$$\text{Absolute radiation dose} = CTDI_{vol} \times \text{Normalized organ dose} \quad (3)$$

Where $CTDI_{vol}$ refers to CT scanner's $CTDI_{vol}$ in a specific protocol and can be planned prior to the examination or extracted from the DICOM images in clinical settings.

## 3.4 | Automatic tube current modulation (ATCM) pilot study—Initial assessment on four cases

The tube current values of each slice are depicted on the red line in Figure 8 where the blue line refers to the average tube current. The normalized fetal dose for these patients from ATCM and FTC examinations were calculated using the developed methodology. That is, the tube current value of each layer was obtained by interpolation, corresponding to simulation calculation settings (just longitudinal (z-) ATCM was accounted for, but no angular tube current modulation), and then the fetal organ dose was calculated. In order to compare the effect of ATCM on fetal dose, the relative deviation between ATCM and FTC was calculated, and the results are shown in Table 4. The tube current is higher than the average value in the scan range of the fetus for patients MAM-16 and MAM-18 as well as the fetal head region of patient MAM-28, which resulted in a higher radiation dose when using ATCM to the fetus of patients MAM-16 and MAM-18 as well as the fetal brain and eyes of patient MAM-28 compared to the FTC protocol. Moreover, the larger size and higher ratio of the visceral belly fat in patients MAM-16 and MAM-18 may result in an increase of tube current when using ATCM at the location of the fetus, leading to increased fetal organ doses.

This study included the largest patients' population covering the whole gestational period using state-of-the-art CT scanners. The mean absolute fetal dose was 0.72 mGy for the Siemens SOMATOM Force using a low-dose ATCM protocol, 13.87 mGy for the Philips Brilliance 40 using a standard ATCM protocol, 13.73 mGy for the Siemens Definition AS using a standard ATCM protocol, and 1.64 mGy for the GE LightSpeed VCT and

**TABLE 3** Normalized organ-level radiation dose estimation models to the fetus with Model I: Normalized organ dose = $\alpha + \beta_1 \times$ MAC + $\beta_2 \times$ GA and Model II: Normalized organ dose = $\alpha + \beta_1 \times$ MAC + $\beta_2 \times$ GA + $\beta_3 \times FD_{skin}$. ($R^2$ refers to the coefficient of determination R-squared).

| Fetal tissue/Organs | | Coefficient | | | | |
|---|---|---|---|---|---|---|
| | | $\alpha$ | $\beta 1$ | $\beta 2$ | $\beta 3$ | $R^2$ |
| Brain | Model I | 1.536 | −0.008 | −0.005 | – | 0.807 |
| | Model II | 1.521 | −0.007 | −0.007 | −0.002 | 0.775 |
| Skeleton | Model I | 6.163 | −0.299 | −0.029 | – | 0.822 |
| | Model II | 5.467 | −0.021 | −0.025 | −0.008 | 0.894 |
| Bone marrow | Model I | 3.354 | −0.016 | −0.024 | – | 0.826 |
| | Model II | 2.702 | −0.010 | −0.016 | −0.005 | 0.837 |
| Soft tissue | Model I | 1.392 | −0.007 | 0.001 | – | 0.723 |
| | Model II | 1.305 | −0.005 | −0.001 | −0.003 | 0.849 |
| Esophagus | Model II | 1.224 | −0.005 | −0.002 | −0.002 | 0.813 |
| Eyes | Model I | 1.339 | −0.007 | −0.003 | – | 0.731 |
| | Model II | 1.359 | −0.009 | 0.001 | 0.001 | 0.669 |
| Thyroid | Model II | 1.566 | −0.009 | 0.000 | −0.001 | 0.802 |
| Spinal cord | Model II | 1.360 | −0.005 | −0.005 | −0.003 | 0.777 |
| Lungs | Model I | 1.420 | −0.007 | −0.002 | – | 0.737 |
| | Model II | 1.266 | −0.005 | −0.001 | −0.003 | 0.822 |
| Heart | Model I | 1.417 | −0.007 | −0.003 | – | 0.773 |
| | Model II | 1.312 | −0.006 | −0.002 | −0.002 | 0.785 |
| Kidneys | Model I | 1.445 | −0.008 | 0.003 | – | 0.526 |
| | Model II | 1.286 | −0.005 | 0.004 | −0.003 | 0.599 |
| Liver | Model I | 1.394 | −0.007 | 0.000 | – | 0.697 |
| | Model II | 1.293 | −0.005 | 0.001 | −0.001 | 0.732 |
| Stomach | Model 1 | 1.366 | −0.007 | 0.000 | – | 0.544 |
| Gall bladder | Model I | 1.230 | −0.006 | 0.001 | – | 0.606 |
| | Model II | 1.193 | −0.005 | −0.001 | −0.001 | 0.556 |
| Sliver Grand | Model I | 1.348 | −0.007 | −0.003 | – | 0.801 |
| | Model II | 1.319 | −0.007 | −0.002 | −0.001 | 0.798 |
| LI | Model 1 | 1.309 | −0.006 | 0.001 | – | 0.549 |
| SI | Model I | 1.344 | −0.007 | 0.001 | – | 0.549 |
| | Model II | 1.318 | −0.005 | −0.002 | −0.002 | 0.522 |
| Skin | Model I | 1.407 | −0.007 | 0.002 | – | 0.732 |
| | Model II | 1.354 | −0.005 | 0.000 | −0.003 | 0.888 |
| Adrenal | Model I | 1.306 | −0.007 | 0.000 | – | 0.626 |
| | Model II | 1.160 | −0.004 | 0.000 | −0.003 | 0.708 |
| Pancreas | Model 1 | 1.327 | −0.007 | 0.001 | – | 0.530 |
| Thymus | Model I | 1.312 | −0.007 | −0.003 | – | 0.801 |
| | Model II | 1.249 | −0.006 | −0.002 | −0.001 | 0.813 |
| Other organs[a] | Model I | 1.371 | −0.007 | −0.001 | – | 0.543 |
| Total body | Model I | 1.716 | −0.010 | 0.012 | – | 0.532 |
| | Model II | 2.519 | −0.012 | −0.010 | −0.001 | 0.919 |

[a]Other organs are all organs of the fetus except the skeleton and bone marrow.

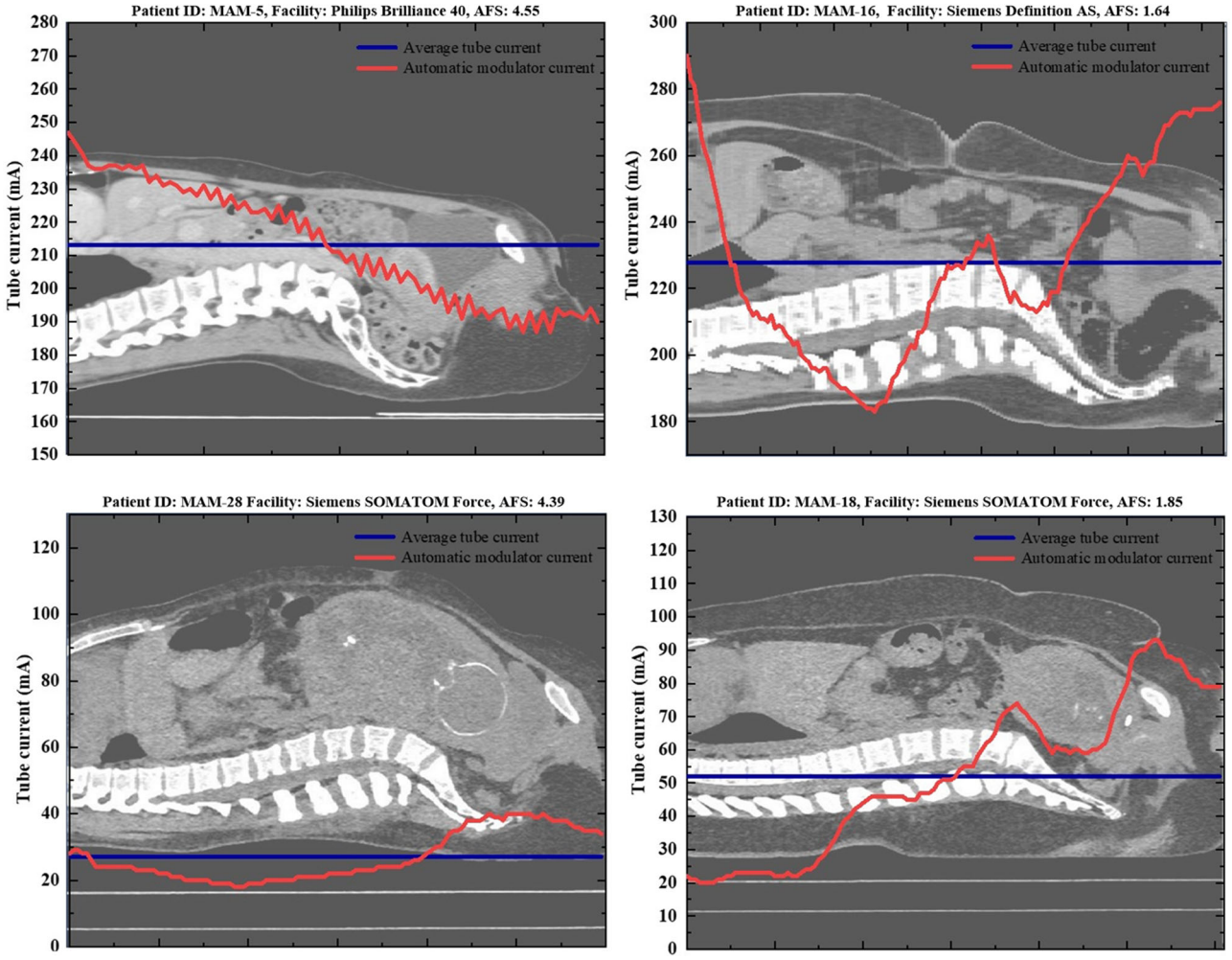


**FIGURE 8** Automatic tube current modulation in real-world abdominal and pelvic CT examinations for the studied pregnant patients.

GE Discovery CT750 HD using a low-dose FTC protocol, respectively.

## 4 | DISCUSSION

In this work, three CT scanner systems were utilized for the estimation of fetal dose in 44 pregnant patients undergoing abdominal/pelvic CT examinations. The average fetal radiation dose per 100 mAs from the FTC protocol was determined to be 7.16 mGy/100 mAs within the range of 4.24-9.81 mGy/100 mAs. The absolute fetal radiation dose varied from 0.72 to 13.87 mGy across different imaging protocols for the investigated pregnant patients at ATCM. Since the fetus has high radiosensitivity and conceptus radiation dose is correlated with childhood cancer after birth, accurate and clinically feasible estimation of fetal organ absorbed doses are crucial in radiological imaging of pregnant female patients. The existing studies mostly reported the radiation dose to fetal total body based on simplified fetus model. In this work, we (i) constructed individual fetus models for each pregnant patient based on corresponding medical images, (ii) calculated fetal organ radiation dose using three CT scanner systems, (iii) analyzed the relationship between the fetal organ dose and various anatomical parameters, and (iv) proposed two computational models for dose estimation of fetal organs from abdominal and pelvic CT examinations.

In addition, we compared the fetal organ dose between various scanning protocols on different CT scanners from the major vendors. We observed that the ATCM technique does not necessarily lead to dose reduction to fetal organs, which we suspect is correlated with the location of fetal organs.

With the use of our newly developed computational models, we found that overall, fetal organ radiation dose decreases with increasing gestational age. As known, in the first trimester, a fetus is highly radiosensitive and would have the highest absorbed dose from CT examinations. Our results showed that the normalized fetal organ dose negatively correlated with MAC, GA, and

**TABLE 4** Comparison of organ dose between automatic tube current modulation and fixed tube current for pregnant patients.

| Tissue/ Organs | Patient ID | | | |
|---|---|---|---|---|
| | MAM-5 | MAM-16 | MAM-18 | MAM-28 |
| Fetal soft tissue | −4.44% | 7.84% | 24.49% | −2.63% |
| Fetal skeleton | −4.02% | 8.15% | 26.26% | 11.52% |
| Fetus Bone Marrow | −4.59% | 7.66% | 27.40% | 18.67% |
| Fetus Brain | −4.76% | 7.95% | 29.46% | 26.54% |
| Fetus Eyes | −4.08% | 8.65% | 28.78% | 18.44% |
| Fetus Lungs | −4.34% | 7.33% | 23.51% | 2.29% |
| Fetus Heart | −4.19% | 7.91% | 24.30% | 2.83% |
| Fetus Kidneys | −3.98% | 7.29% | 22.06% | −9.04% |
| Fetus Liver | −3.94% | 7.54% | 22.50% | −7.15% |
| Fetus Stomach | −4.10% | 8.20% | 23.71% | −7.75% |
| Fetus Gall bladder | −3.95% | 7.44% | 21.61% | −11.32% |
| Fetus Salivary Grand | −4.31% | 8.30% | 25.59% | 16.48% |
| Fetus LI | −3.77% | 8.12% | 23.08% | −12.07% |
| Fetus SI | −3.89% | 8.11% | 22.79% | −11.72% |
| Fetus UB | −3.63% | 7.80% | 22.57% | −13.90% |
| Fetus Adrenal | −4.05% | 7.47% | 22.26% | −6.85% |
| Fetus Pancreas | −3.80% | 7.61% | 22.54% | −12.29% |
| Fetus Spleen | 3.15% | 8.66% | 23.91% | −8.78% |
| Fetus Thymus | 17.81% | 8.07% | 24.36% | 6.40% |
| Average | −2.57% | 7.90% | 24.27% | −0.02% |

FDs, but weak correlation was found with FL, HL, HC, BPD, FAC, and scan length. The absorbed dose to the fetal skeleton was shown to be significantly higher than bone marrow and other organs. This is mainly due to the higher density of the skeleton, which results in the absorption of more scattered radiation. Therefore, prior to performing radiological imaging procedures on pregnant females, the radiologist may give special consideration to the absorbed dose and radiation risks to the fetal skeleton and bone marrow, especially in the first trimester.

The effect of ATCM on fetal radiation dose is rarely discussed and is often overlooked. In our study, the tube current modulation schemes of ATCM extracted from DICOM images of various pregnant patients from different CT scanners were reported. In some cases, ATCM did not improve dose savings to the fetus in pregnant patients and even worse, leads to increased fetal organ dose. For patients MAM-16 and MAM-18, the radiation dose to the fetus when using the ATCM protocol was higher than the one without the FTC protocol. ATCM is aimed to adjust the tube current according to the attenuation characteristics of the patient on the premise of ensuring good image quality as well as reducing the radiation exposure.[27] It has been reported that with the increase of cross-sectional dimensions of patients, the tube current in ATCM will increase accordingly to ensure the quality of CT images and may result in the increase of absorbed dose.[28] Hence, we compared the abdominal size of these patients by measuring the abdominal fat ratio (AFS) values,[29] which refers to the distance from the anterior spine to the anterior abdominal wall divided by the maximum distance from the outer edge of the rectus sheath to the dermis in the same CT image. To some extent, AFS also indicates the fat layer thickness/body circumference of a pregnant woman during pregnancy. The calculated AFS values for patients MAM-5, MAM-16, MAM-18, and MAM-28 were 4.55, 1.64, 1.85, and 4.39, respectively. The lower AFS for MAM-16 and MAM-18 indicated the higher rate of visceral belly fat and may result in an increase of tube current and absorbed radiation dose to the fetus when using the ATCM protocol.

Table 5 compares the reported fetal radiation dose from CT examinations between this study and the existing literatures[4,6,10,15,21–25] along with the current modulation mode (ATCM/FTC), patient number, CT protocol number, and gestational age. As shown in Table 5, the calculated fetal doses from this work were lower than the values reported by Hardy et al.,[10] which can be mainly attributed to the differences in CT scanners and the computational pregnant female phantoms. The absorbed fetal dose to patients undergoing CT examinations using the Siemens SOMATOM Force was found to be as low as $0.72 \pm 0.81$ mGy, which is due to the low tube current and $CTDI_{vol}$ of the chosen protocol. For FTC in two GE CT scanners, the absolute fetal radiation dose was found to be lower than that reported in the literature, which can be attributed to the use of a low-dose scanning protocol, different CT scanners, and individual differences among pregnant patient models. The fetal absorbed dose for all investigated patients in this study were shown to be far below the minimum negligible risk level of 50 mGy for pregnant female receiving a single radiological diagnostic imaging procedure. However, when repeated standard dose CT examinations are needed for pregnant patients in the clinical setting, the accumulated fetal dose may lead to non-negligible radiation hazard and cancer risks for the developing fetus and after-birth child.

This study inherently bears some limitations. Due to the use of low-dose scanning protocols for pregnant patients, most of the fetal internal soft-tissues are difficult to segment within the CT images. The approximation of using the developed anchor phantom and the reference fetal developing measurements provided by the WHO and ICRP may introduce individual uncertainties for radiation dose calculations to these organs. This is a pilot study focusing on an initial assessment of four cases. The patient population evaluated in this work with respect to ATCM needs to be expanded further to include more generalized patterns of CT scanners and scanning protocols. Future work will

**TABLE 5** Comparison of the total-body fetal doses between this work and those reported in the literature.

| | No. of patients | No. of real CT protocol/ company[h] | Range of gestational age | Current modulation mode | Fetal radiation dose (mGy) | | Fetal radiation dose per 100 mAs (mGy/100 mAs) | | Fetal radiation dose per $CTDI_{vol}$ | |
|---|---|---|---|---|---|---|---|---|---|---|
| | | | | | Average ± SD | Range | Average ± SD | Range | Average ± SD | Range |
| This study | 44 | 5/3 | 8~35 weeks | ATCM[f] | 0.72 ± 0.81[a], 13.87[b], 13.73[c] | 0.39~13.87 | 7.38 ± 2.61 | 6.54~9.11 | 0.95 ± 0.49 | 0.84~1.17 |
| | | | | FTC | 1.64 ± 0.33[d,e] | 0.97~2.24 | 7.16 ± 1.66 | 4.24~9.81 | 0.95 ± 0.25 | 0.56~1.30 |
| Hardy et al.[10,21] | 24 | 6/1 | 5~36 weeks | ATCM[g] | 16.61 ± 4.10 | 10.86~22.39 | – | – | 1.43 ± 0.24 | 1.09~1.87 |
| | | | | FTC | 21.30 ± 5.26 | 14.87~28.12 | – | – | 1.37 ± 0.26 | 0.96~1.81 |
| Matsunaga et al.[22] | 1 | 0 | 30 weeks | FTC | 2.93 ± 0.41 | 2.5~3.3 | – | – | – | – |
| Xie et al.[4] | 30 | 1/1 | 8~35 weeks | FTC | – | – | 9.20 ± 1.60 | 6.70~13.0 | 1.17 ± 0.20 | 0.85~1.63 |
| Gu et al.[6] | 3 | 0 | 3, 6, 9 months | FTC | 12.22 ± 8.00 | 7.81~20.92 | 6.90 | – | – | – |
| Matsunaga et al.[23] | 1 | 2/1 | 30 weeks | FTC | 3.1 | – | – | – | – | – |
| Damilakis et al.[24] | 117 | 1/1 | 0~7 weeks | FTC | – | – | – | – | 0.62 ± 0.29 | |
| Angel et al.[15] | 24 | 6/1 | 5~36 weeks | FTC | – | – | 11.06 ± 2.24 | 9.51~14.52 | – | – |
| Felmlee et al.[25] | 1 | 4/3 | – | FTC | – | – | 11.30 | 9.00~13.60 | – | – |

[a] Siemens SOMATOM Force: collimator = 57.6 mm, tube voltage = 120 kVp, mean effective mAs = 22.17 (MAM-28) / 43.03 (MAM-18), table feed per rotation = 34.5 mm/s, pitch = 0.60.
[b] Philips Brilliance 40: collimator = 40 mm, tube voltage = 120 kVp, mean effective mAs = 162.51, table feed per rotation = 52.5 mm/s, pitch = 0.656.
[c] Siemens Definition AS: collimator = 19.2 mm, tube voltage = 120 kVp, mean effective mAs = 141.93, table feed per rotation = 15.4 mm/s, pitch = 0.80.
[d] GE LightSpeed VCT: collimator = 40 mm, tube voltage = 120 kVp, mean effective mAs = 22.9, table feed per rotation = 55 mm/s, pitch = 1.375.
[e] GE Discovery CT750 HD: collimator = 40 mm, tube voltage = 120 kVp, mean effective mAs = 22.88, table feed per rotation = 55 mm/s, pitch = 1.375.
[f] Patient-specific tube current modification extracted from DICOM header of patient.
[g] Simulated tube current.
[h] Number of CT scans performed on patients, "0" represents the reference phantom used.

report on the generation of tube current modification pattern of the ATCM protocol to reduce fetal radiation dose.

## 5 | CONCLUSION

A clinically feasible framework for calculation of fetal organ-level radiation dose from abdominal and pelvic CT examinations was developed based on personalized computational phantoms of a series of fetus representative of a comprehensive range of gestational age, maternal size, and fetal anatomical characteristics. Fetal organ radiation doses were calculated for three CT scanner systems using validated Monte Carlo simulations. The correlation between fetal organ doses and anatomical parameters, fetal developing indicators, and clinical scanning protocols was investigated. The use of ATCM for abdominal and pelvic CT scanning on pregnant patients was also investigated indicating that it may not lead to radiation dose savings for the fetus.

### ACKNOWLEDGMENTS

This work was supported by National Natural Science Foundation of China (32227801) and the Swiss National Science Foundation under grant SNSF 320030_176052.

### CONFLICT OF INTEREST STATEMENT

The authors declare no conflicts of interest.

### REFERENCES

1. Osei EK, Faulkner K. Fetal doses from radiological examinations. *Br J Radiol*. 1999;72(860):773-780.
2. ICRP. Publication 84:Pregnancy and Medical Radiation. Annals of the ICRP. 2000.
3. ICRP. Publication 103: the 2007 recommendations of the international commission on radiological protection. *Ann ICRP*. 2007;37.
4. Xie T, Poletti PA, Platon A, Becker CD, Zaidi H. Assessment of CT dose to the fetus and pregnant female patient using patient-specific computational models. *Eur Radiol*. 2018;28(3):1054-1065.
5. Gu J, Bednarz B, Caracappa P, Xu X. The development, validation and application of a multi-detector CT (MDCT) scanner model for assessing organ doses to the pregnant patient and the fetus using Monte Carlo simulations. *Phys Med Biol*. 2009;54(9):2699.
6. Gu J, Xu XG, Caracappa PF, Liu B. Fetal doses to pregnant patients from CT with tube current modulation calculated using Monte Carlo simulations and realistic phantoms. *Radiat Prot Dosim*. 2013;155(1):64-72.
7. Xu XG, Taranenko V, Zhang J, Shi C. A boundary-representation method for designing whole-body radiation dosimetry models: pregnant females at the ends of three gestational periods—RPI-P3, -P6 and -P9. *Phys Med Biol*. 2007;52(23):7023-7044.
8. Motavalli LR, Azghadi EH, Hakimabad HM, Akhlaghi P. Pulmonary embolism in pregnant patients: assessing organ dose to pregnant phantom and its fetus during lung imaging. *Med Phys*. 2017;44(11):6038-6046.
9. Hoseinian E, Motavalli LR, Hakimabad HM. Hybrid pregnant reference phantom series based on adult female ICRP reference phantom. *Radiat Phys Chem*. 2018;144.
10. Hardy AJ, Bostani M, Angel E, Cagnon C, Sechopoulos I, McNitt-Gray MF. Reference dataset for benchmarking fetal doses derived from Monte Carlo simulations of CT exams. *Med Phys*. 2021;48(1):523-532.
11. Maynard MR, Geyer JW, Aris JP, Shifrin RY, Bolch W. The UF family of hybrid phantoms of the developing human fetus for computational radiation dosimetry. *Phys Med Biol*. 2011;56(15):4839-4879.
12. ICRP. Publication 145: Adult Mesh-Type Reference Computational Phantoms [published online ahead of print 2020/11/25]. *Ann ICRP*. 2020;49.
13. Xie T, Zaidi H. Development of computational pregnant female and fetus models and assessment of radiation dose from positron-emitting tracers. *Eur J Nucl Med Mol Imaging*. 2016;43(11):2290-2300.
14. Xie T, Zaidi H. Estimation of the radiation dose in pregnancy: an automated patient-specific model using convolutional neural networks. *Eur Radiol*. 2019;29(12):6805-6815.
15. Angel E, Wellnitz CV, Goodsitt MM, et al. Radiation dose to the fetus for pregnant patients undergoing multidetector CT imaging: monte Carlo Simulations estimating fetal dose for a range of gestational age and patient size1. *Radiology*. 2008;249(1):220-227.
16. Qu SY, Xie TW, Giger ML, Mao XQ, Zaidi H. Construction of a digital fetus library for radiation dosimetry. *Med Phys*. 2023;50(4):2577-2589.
17. Akbarzadeh A, Ay MR, Ghadiri H, Sarkar S, Zaidi H. Measurement of scattered radiation in a volumetric 64-slice CT scanner using three experimental techniques. *Phys Med Biol*. 2010;55(8):2269-2280.
18. Akhavanallaf A, Xie T, Zaidi H. Assessment of uncertainties associated with Monte Carlo-based personalized dosimetry in clinical CT examinations [published online ahead of print 2020/01/15]. *Phys Med Biol*. 2020;65(4):045008.
19. Yang Y, Zhuo W, Zhao Y, Xie T, Wang C, Liu H. Estimating specific patient organ dose for chest ct examinations with monte carlo method. *Appl Sci*. 2021;11(19):8961.
20. Waters LS, McKinney GW, Durkee JW, et al. The MCNPX Monte Carlo radiation transport code. Paper presented at: AIP conference Proceedings 2007.
21. Hardy AJ, Angel E, Bostani M, Cagnon C, McNitt-Gray M. Estimating fetal dose from tube current-modulated (TCM) and fixed tube current (FTC) abdominal/pelvis CT examinations. *Med Phys*. 2019;46(6):2729-2743.
22. Matsunaga Y, Kawaguchi A, Kobayashi M, et al. Fetal dose conversion factor for fetal computed tomography examinations: a mathematical phantom study. *J Appl Clin Med Phys*. 2017;18(5):330-335.
23. Matsunaga Y, Kawaguchi A, Kobayashi M, Suzuki S, Suzuki S, Chida K. Radiation doses for pregnant women in the late pregnancy undergoing fetal-computed tomography: a comparison of dosimetry and Monte Carlo simulations. *Radiol Phys Technol*. 2017;10(2):148-154.
24. Damilakis J, Perisinakis K, Tzedakis A, Papadakis AE, Karantanas A. Radiation dose to the conceptus from multidetector CT during early gestation: a method that allows for variations in maternal body size and conceptus position. *Radiology*. 2010;257(2):483-489.
25. Felmlee JP, Gray JE, Leetzow ML, Price JC. Estimated fetal radiation-dose from multislice CT studies. *Am J Roentgenol*. 1990;154(1):185-190.
26. Turner AC, Zankl M, Demarco JJ, et al. The feasibility of a scanner-independent technique to estimate organ dose from MDCT scans: using CTDIvol to account for differences between scanners. *Med Phys*. 2010;37(4):1816-1825.
27. Kalra MK, Maher MM, Toth TL, et al. Techniques and applications of automatic tube current modulation for CT [published online ahead of print 2004/10/23]. *Radiology*. 2004;233(3):649-657.
28. Qurashi AA, Rainford LA, Alshamrani KM, Foley SJ. The impact of obesity on abdominal CT radiation dose and image quality. *Radiat Prot Dosim*. 2019;185(1):25-34.

29. Scott SI, Farid S, Mann C, Jones R, Evans J. Abdominal fat ratio - A novel parameter for predicting conversion in laparoscopic colorectal surgery. *Ann R Coll Surg Engl*. 2016;99(1):1-5.

## SUPPORTING INFORMATION

Additional supporting information can be found online in the Supporting Information section at the end of this article.

**How to cite this article:** Qu S, Liu H, Xie T, Giger ML, Quan G, Zaidi H. Patient-specific fetal radiation dosimetry for pregnant patients undergoing abdominal and pelvic CT imaging. *Med Phys*. 2023;50:3801–3815. https://doi.org/10.1002/mp.16304